

# A Study of Busemann-type Biplane for Avoiding Choked Flow

H. Yamashita<sup>\*</sup>, M. Yonezawa<sup>†</sup> and S. Obayashi<sup>‡</sup>  
*Tohoku University, Sendai, Japan, 980-8577*

and

K. Kusunose<sup>§</sup>

*Formerly Institute of Fluid Science, Tohoku University and Currently Technical Research and Development  
Institute, Japan Defense Agency, Tokyo, Japan, 190-8533*

**This study establishes methods to overcome choked-flow and flow-hysteresis problems of Busemann biplane at off-design conditions. Two-dimensional (2-D) analyses of three Busemann-type biplanes have been addressed, using the application of Computational Fluid Dynamics (CFD) code in inviscid flow (Euler) mode. These biplane configurations are designed in such a way that the front streamline area and the rear streamline area can be changed with the use of leading- and trailing-edge flaps (similar to high-lift devices). In this paper, the individual effects of the change in each area on choked-flow and flow-hysteresis are studied in detail. Also, the combined effect of the two is investigated. The results of these analyses show the solutions that are highly capable of overcoming these problems.**

## Nomenclature

$A_i$	=	area of inlet
$A_t$	=	area of throat
$C_d$	=	wave drag coefficient
$C_p$	=	pressure coefficient
$c$	=	chord
$M_\infty$	=	free-stream Mach number
$t$	=	airfoil thickness
$\beta$	=	shock-wave angle
$\gamma$	=	ratio of specific heats
$\varepsilon$	=	wedge angle of Busemann biplane

## I. Introduction

In 2003, the first and last supersonic transport (SST), the Concorde (1969~2003), had finished its flight services, before completing a development of next-generation SST. Hence, every commercial airplane flies at transonic speed now. It is important to note that the Concorde had already flown for as long as 30 years, although our aviation history is only about 100 years. These 30 years of flight are truly admirable achievement and have given us great knowledge, technologies and significant challenges.

An important problem that needs to be overcome is the sonic boom generated by shock waves from an airplane flying at supersonic speed. In our research, we have studied a biplane concept proposed by Kusunose<sup>1,2</sup> that will enable a significant reduction, if not complete elimination, of shock waves. Fundamentally, for two-dimensional airfoils, wave drag may be separated into drag due to lift (including the camber effect of the airfoils) and drag due to thickness in supersonic flow<sup>3</sup>. In spite of the fact that wave drag due to lift cannot be eliminated completely, it can be reduced significantly by using multi-airfoil configurations. These configurations re-distribute the system's total lift among the individual airfoil elements, reducing the lift of each individual element and the total wave drag of the system. We call this the "wave reduction effect". In the same way, the wave drag due to thickness can also be almost

---

<sup>\*</sup> Graduate student, Institute of Fluid Science, Student Member AIAA.

<sup>†</sup> Graduate student, Institute of Fluid Science, Student Member AIAA.

<sup>‡</sup> Professor, Institute of Fluid Science, Member AIAA.

<sup>§</sup> Senior Research Scientist, Japan Defense Agency, Member AIAA.

eliminated by using a biplane configuration, which depends on mutual cancellation of waves between the two airfoil elements. This will be referred to as the “wave cancellation effect” hereinafter in this paper. For these reasons, an ideal boomless biplane configuration can be designed by applying these two effects<sup>4,5</sup>.

It is, however, difficult to design an ideal boomless biplane that can fly effectively from subsonic to supersonic speed in real flight. The reason for this is that the desired wave cancellation effect, which is based on Busemann biplane, can only be achieved at the designed Mach number and at a specific flow condition. Unfortunately, under off-design conditions, there are choked-flow phenomenon and flow-hysteresis, resulting in a severe drag penalty. Thus the purpose of this study is to formulate how a biplane airfoil, based on Busemann biplane, will be able to overcome a choked-flow and flow-hysteresis under off-design conditions. Figure 1 shows the conceptual drawing of a boomless supersonic transport in flight which is based on our biplane concept.



**Figure 1. Conceptual drawing of boomless supersonic transport in flight.**

## **II. Choked-Flow and Flow-Hysteresis Problems at Off-design Conditions of Busemann Biplane**

Let us begin our analysis by confirming the drag characteristics both of the Busemann biplane and the baseline diamond airfoil over a range of Mach numbers ( $0.3 \leq M_\infty \leq 3.3$ ), using the CFD analyses. Figure 2 shows the configurations of these two airfoils, while Fig. 3 shows the drag characteristics of the two airfoils at a range of Mach numbers. The thickness-chord ratio of Busemann biplane and the diamond airfoil are  $t/c=0.05$  and  $t/c=0.1$  respectively, since it is necessary for these two airfoils to have the same total thickness to simulate equivalent (total) airfoil thickness. The wedge angles of Busemann biplane are therefore 5.7 deg., and the wedge angle of the diamond airfoil is 11.4 deg., which is just twice the angle of Busemann biplane (see Fig. 2, where  $\epsilon$  is the wedge angle of Busemann biplane). The distance between the two biplane elements was 0.5 (when the chord length is 1.0) for a designed Mach number 1.7 to obtain the theoretical minimum drag.

Figure 3 shows that the Busemann biplane, for a wide range of Mach numbers ( $1.64 \leq M_\infty \leq 2.7$ ), has a wave drag lower than that of the diamond airfoil<sup>6,7</sup>. In this low-drag range, the wave cancellation effect is critical and we hope to use this range in real flight. In decelerating condition, however, a high wave drag occurs when Mach number is  $M_\infty=1.63$  because of the appearance of strong bow shock in front of the biplane. This is a choked-flow phenomenon of Busemann biplane. The  $C_p$  distributions of Busemann biplane (including a choked-flow,  $1.5 \leq M_\infty \leq 1.7$ ) are illustrated in detail in Fig. 4. As the Mach number is reduced from its design Mach number ( $M_\infty=1.7$ ), shock waves generated by the elements interact with one another and a subsonic area is formed near the throat of the biplane. Eventually, the flow is choked at the maximum thickness sections between the two elements, and the subsonic area is propagated to upstream, forming a bow shock (see Fig. 4). In accelerating conditions (as shown in Fig. 5), and then, the Busemann biplane has a flow-hysteresis for a range of Mach numbers ( $1.63 \leq M_\infty \leq 2.18$ ). For this reason, the  $C_d$  values of the accelerating and decelerating conditions are not the same. Thus, if we would like to make Busemann biplane reach the design point ( $M_\infty=1.7$ ) from subsonic, it needs to exceed the Mach number of  $M_\infty=2.18$ , where a bow shock is swallowed backward between wing elements.

Taking these into consideration, we need to discover methods that are applicable to a biplane based on a Busemann-type biplane for real flight in order to avoid the choked-flow and flow-hysteresis problems at off-design conditions. Before we examine how these problems can be overcome, it may be useful to discuss the start/un-start characteristics of supersonic inlet diffuser (see Fig. 6), because the phenomena are similar to that of Busemann biplane. In Fig. 6, the line in red shows the Kantrowitz limit<sup>8</sup>, where once the bow shock is generated in front of the

inlets, for the inlets to go from unstart condition to start condition, it has to exceed the mach number set by the Kantrowitz limit (given by Eq. (1)).

$$\frac{A_t}{A_i} = \left[ \frac{(\gamma - 1)M_\infty^2 + 2}{(\gamma + 1)M_\infty^2} \right]^{\frac{1}{2}} \left[ \frac{2\gamma M_\infty^2 - (\gamma - 1)}{(\gamma + 1)M_\infty^2} \right]^{\frac{1}{\gamma - 1}} \quad (1)$$

where  $A_i$  is the area of inlet and  $A_t$  is the area of throat. Also, the line in blue refers to the isentropic contraction limit, where the Mach number is  $M_\infty=1.0$  at the throat of supersonic inlets. The isentropic contraction limit is calculated by Eq. (2).

$$\frac{A_t}{A_i} = M_\infty \left[ \frac{(\gamma - 1)M_\infty^2 + 2}{\gamma + 1} \right]^{-\frac{(\gamma + 1)}{2(\gamma - 1)}} \quad (2)$$

It is reasonable to suppose that this rule is applicable to avoid the choked-flow and flow-hysteresis of Busemann biplane. In fact, the results from CFD analyses are in good agreement with the values which are calculated using Eqs. (1) and (2) (here the  $A_t/A_i$  of Busemann biplane is 0.8, as shown by the solid-line in Fig. 6).

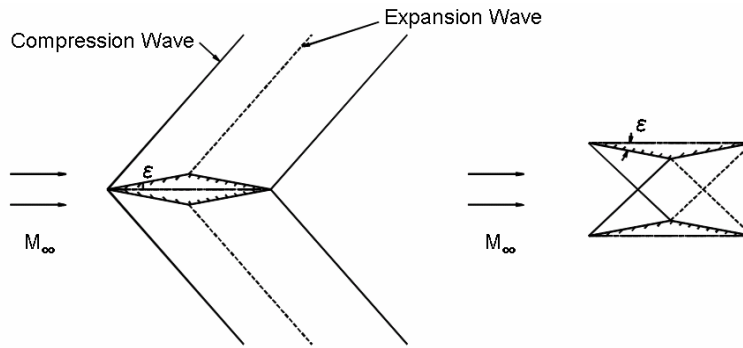


Figure 2. Configuration of both the Busemann biplane ( $t/c=0.05$ ) and the baseline diamond airfoil ( $t/c=0.1$ ).

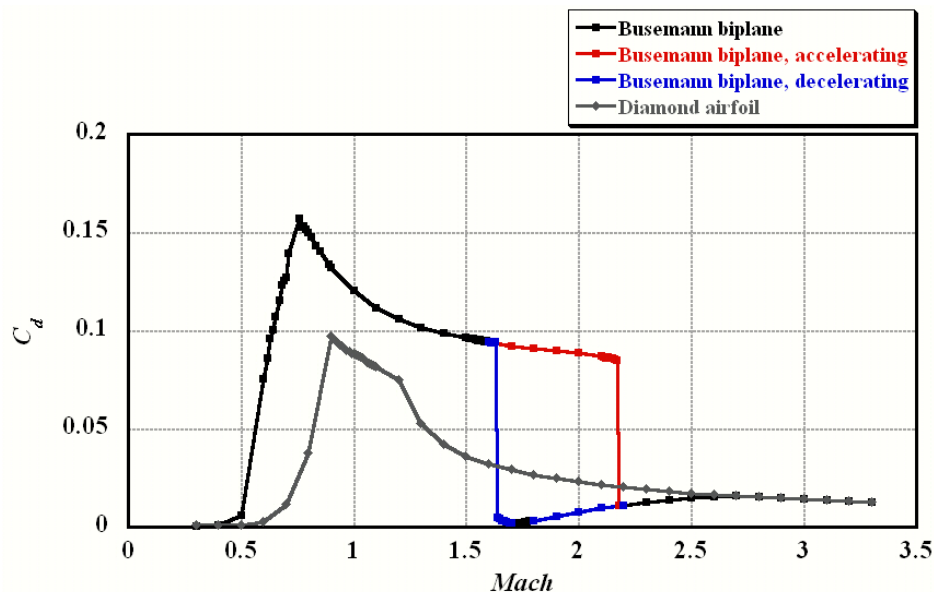


Figure 3. Comparison of the drag characteristics of Busemann biplane and diamond airfoil.

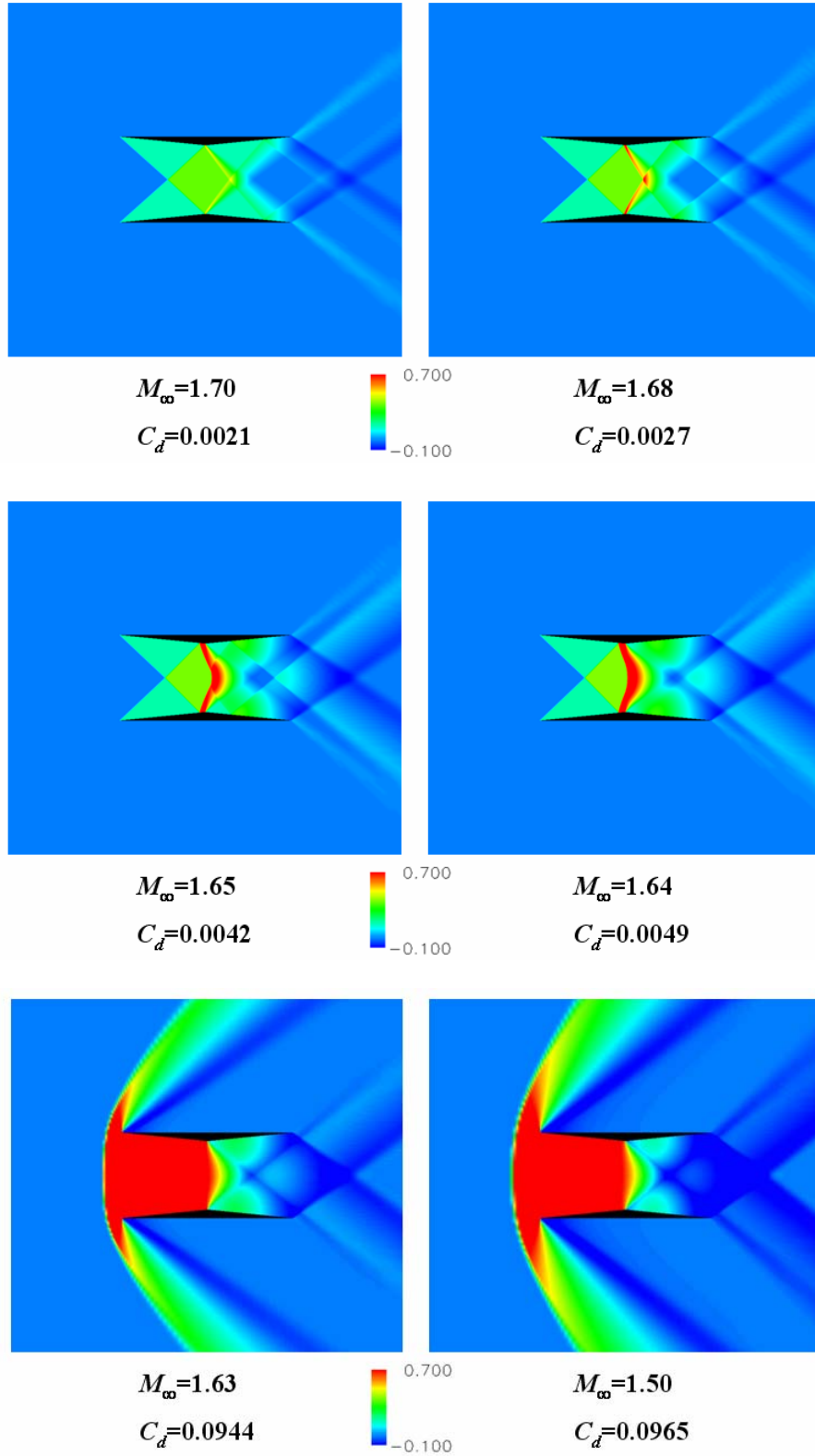


Figure 4.  $C_p$ -contours of Busemann biplane with zero-lift in decelerating condition ( $1.5 \leq M_\infty \leq 1.7$ ).

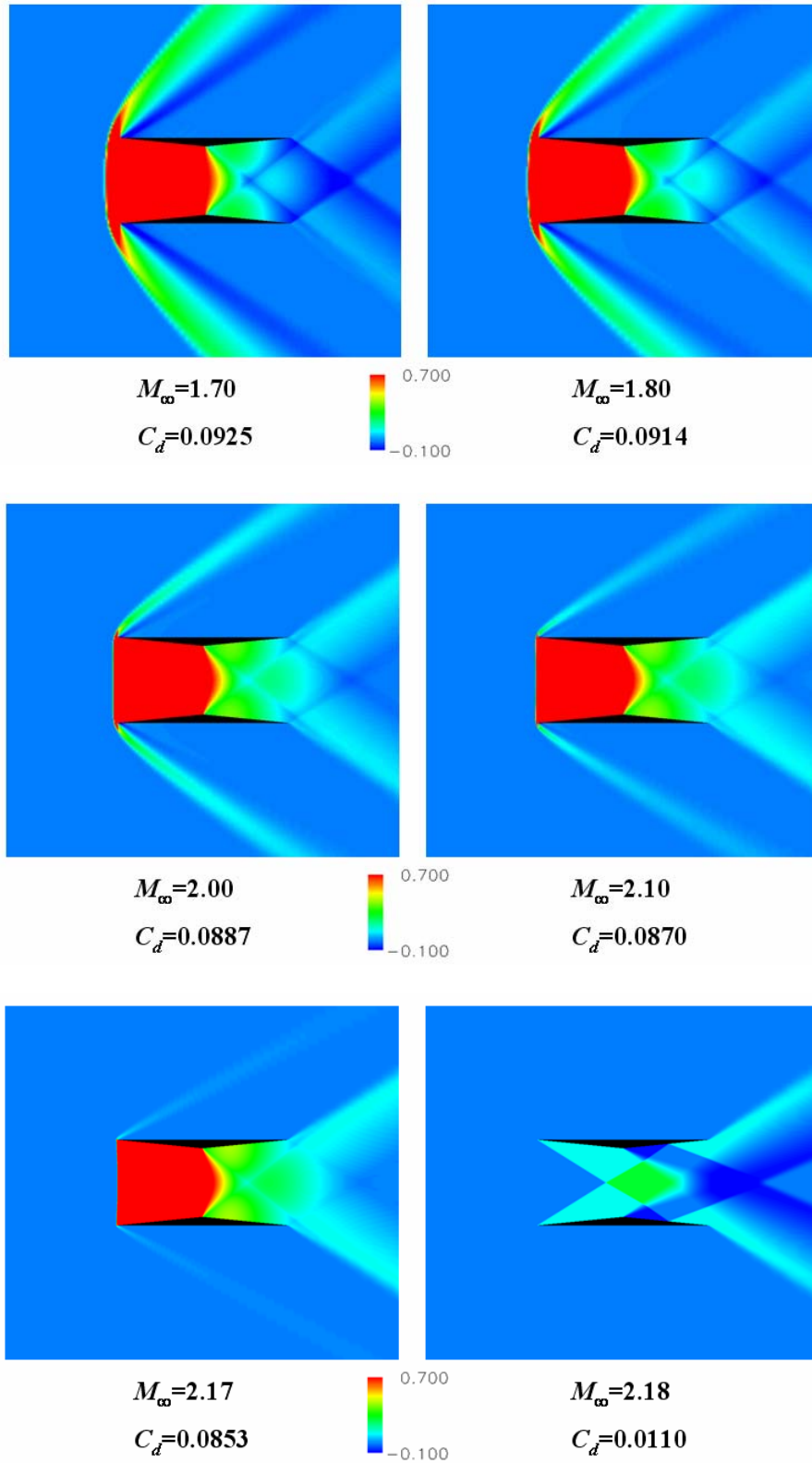


Figure 5.  $C_p$ -contours of Busemann biplane with zero-lift in accelerating condition ( $1.7 \leq M_\infty \leq 2.18$ ).

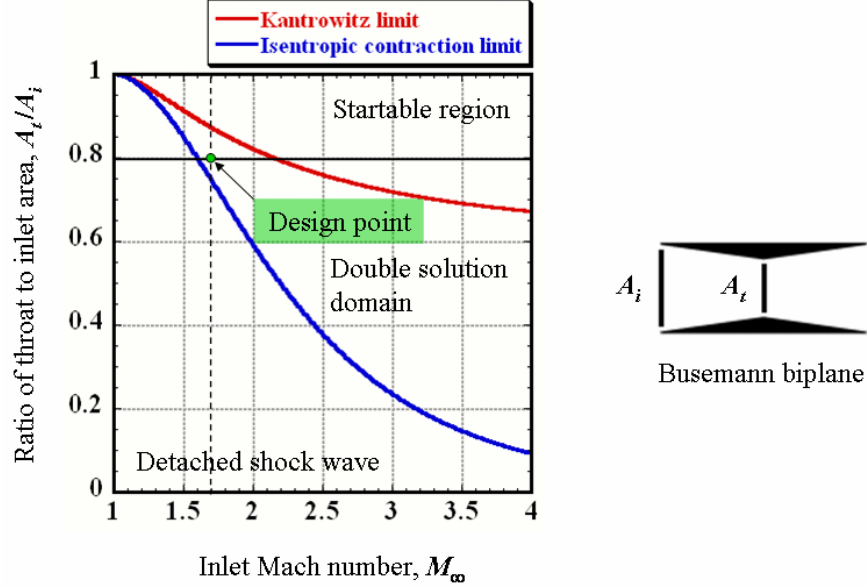


Figure 6. Start/Un-start characteristics of supersonic inlet diffuser.

### III. Results and Discussion

The Euler equation is solved for all configurations by the CFD tool (UPACS<sup>9</sup>) that was developed at the Japan Aerospace Exploration Agency (JAXA), mainly focusing on shock wave properties observed around biplane configurations. The Multiblock method is applied to grid generation in all cases. Here, it is important to note the accuracy of the CFD analysis by using UPACS-code. What has been demonstrated in Refs. 2 and 10 is that the CFD results and analytical results derived from the supersonic thin airfoil theory<sup>3</sup> are in good agreement when comparing configurations, such as a single flat plate airfoil, parallel flat plate airfoils, a diamond airfoil and Busemann biplane. Therefore, we are not concerned here with its validation. The detailed descriptions of the UPACS solvers can be found in Ref. 9. Let us consider in this section the results from CFD analyses for 2-D biplane configurations in inviscid flow, with zero-lift conditions (angle of attack for all configurations are set to zero).

#### A. Diamond Airfoil Separated into Two Elements

The diamond airfoil separated into two elements along the chord length of the baseline diamond airfoil was calculated using the validated UPACS-code in order to start the verification of avoidance of choked-flow and flow-hysteresis. Figure 7 shows the grid structure used for the 2-D analyses. Approximately 0.52 million grid points are used in total. The grid numbers around each biplane element and between these two elements are 750 and 251×251, respectively. Here, thickness-chord ratio ( $t/c$ ) of individual elements was 0.05 (because thickness-chord ratio of the baseline diamond airfoil is 0.1) and the distance between two elements was 0.5 (relative to the chord length is 1.0) respectively. Mach numbers range from 0.3 to 3.3 on the grounds that an airplane has to fly subsonic, transonic and supersonic in real flight. The drag characteristics of this biplane are plotted in Fig. 8, which also includes the drag characteristics of Busemann biplane and the baseline diamond airfoil (given in Fig. 3).

It is clear that the wave drag of the diamond airfoil separated into two elements agree very well with that of the baseline diamond airfoil at all Mach numbers. The choked-flow and flow-hysteresis do not exist in all Mach numbers, assuming that the area of streamline has not changed. Therefore, these facts suggest that it is possible to avoid a choked-flow and flow-hysteresis of Busemann biplane by bringing Busemann biplane close to the shape of the diamond airfoil separated into two elements. In light of limits shown in Fig. 6, these results are credible since the ratio of throat-to-inlet-area of diamond airfoil separated into two elements is  $A_t/A_i=1.0$ . Pressure contours of this biplane at Mach number  $M_\infty=1.5$  are given in Fig. 9. From Fig. 9, we can confirm that a bow shock is generated at the upstream of Busemann biplane; in contrast, there is no choked-flow phenomenon at the diamond airfoil separated into two elements.

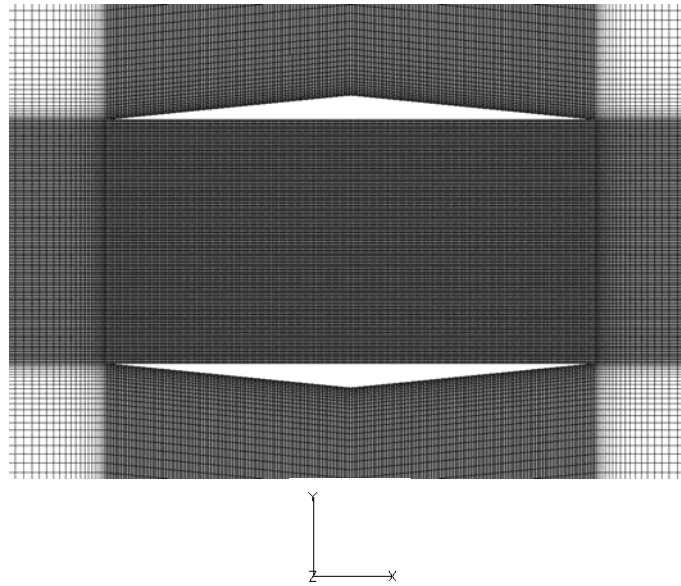


Figure 7. Near-field grids of diamond airfoil separated into two elements used for UPACS-code analyses.

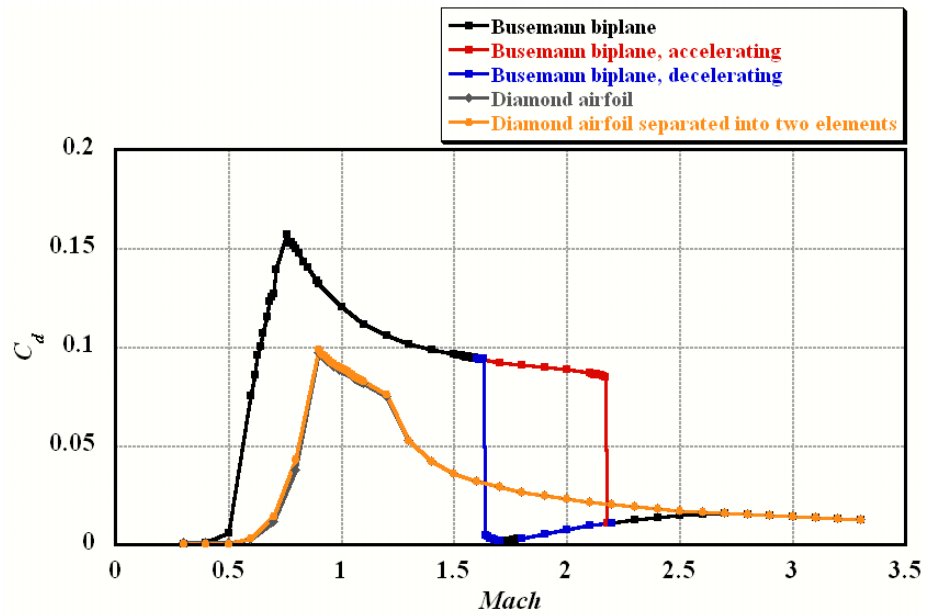


Figure 8. Comparison of the drag characteristics among Busemann biplane, diamond airfoil and diamond airfoil separated into two elements.

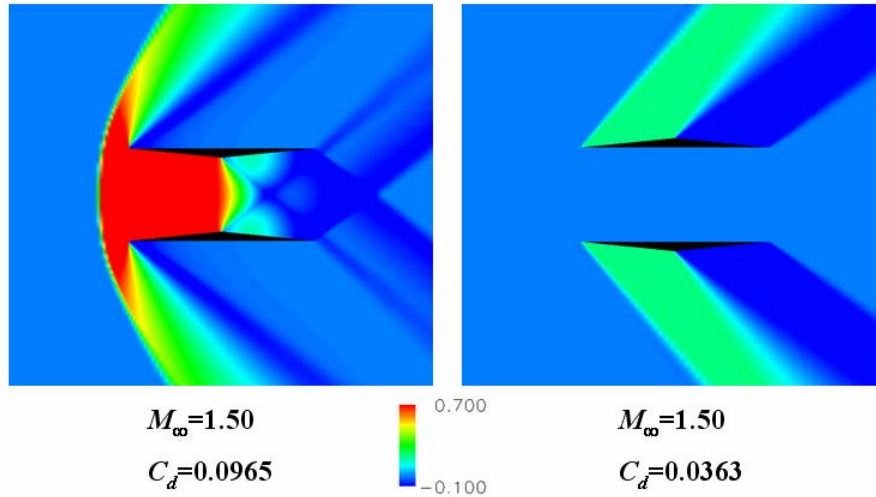


Figure 9.  $C_p$ -contours of Busemann biplane and diamond airfoil separated into two elements with zero-lift ( $M_\infty=1.5$ ).

### B. Busemann Biplane with Deflected Leading-edge Flaps

In order to examine the effect of change in the area of front streamline on choked-flow and flow-hysteresis, Busemann biplane with deflected leading-edge flaps (as sketched in Fig. 10) was calculated using UPACS-code by considering flow-hysteresis. This biplane is actually a deflected Busemann biplane, whereby 28% of the parts from the leading-edges of the Busemann biplane ( $t/c=0.05$ ) are moved inward to become something similar to high-lift devices used at takeoff and landing conditions. The inner sides of the deflected parts become parallel to each other, and uniform flow is undisturbed between them. In supersonic flow, therefore, oblique shock wave is generated at 28% position among the two elements, then the oblique shock waves meet the vertex of a triangle of the other element at  $M_\infty=1.3$  (the wave angle is about  $\beta = 63$  deg. at  $M_\infty=1.3$ , see in Fig. 10). Mach numbers range from 0.3 to 3.3 in inviscid flow mode. Figure 11 shows the near-field grids and the drag characteristics of the biplane are plotted in Fig. 12, which includes those of Busemann biplane and the baseline diamond airfoil (given in Fig. 3). Pressure coefficient contours around the biplane are plotted in Figs. 13 and 14 with a change in free-stream Mach number.

It is found from Fig. 12 that the increase in the drag of the biplane due to choked-flow becomes small, in contrast to that of Busemann biplane. In addition, the change in the area of front streamline enables the shift of the Mach number at which the flow is choked at the maximum thickness sections between the two elements to a lower Mach number  $M_\infty=1.41$  (in the case of Busemann biplane,  $M_\infty=1.63$ ), propagating the subsonic area to upstream, forming a bow shock. Also, the area of flow-hysteresis is reduced compared to that of Busemann biplane, where the bow shock that is generated in front of leading-edges is swallowed at Mach number  $M_\infty=1.61$ . It follows from this that the effect with leading-edge flaps can downscale the wave drag in supersonic flow condition, and also some range of subsonic flow conditions. In light of limits shown in Fig. 6, these results are in good agreement with the values theoretically (note that the ratio of throat-to-inlet-area of Busemann biplane with deflected leading-edge flaps is about  $A_t/A_i=0.9$ ).

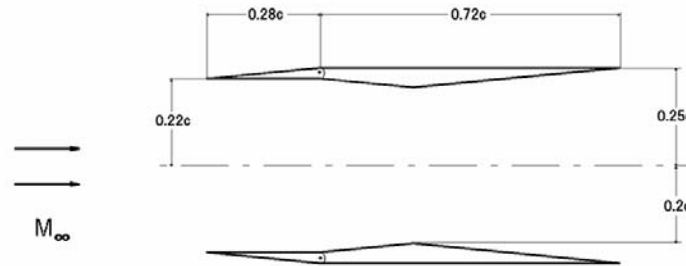


Figure 10. Configuration of Busemann biplane with deflected leading-edge flaps.

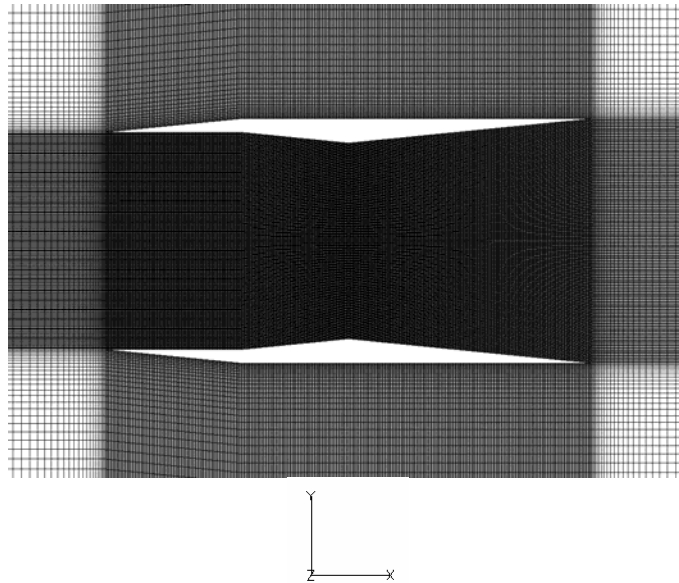


Figure 11. Near-field grids of Busemann biplane with deflected leading-edge flaps used for UPACS-code analyses.

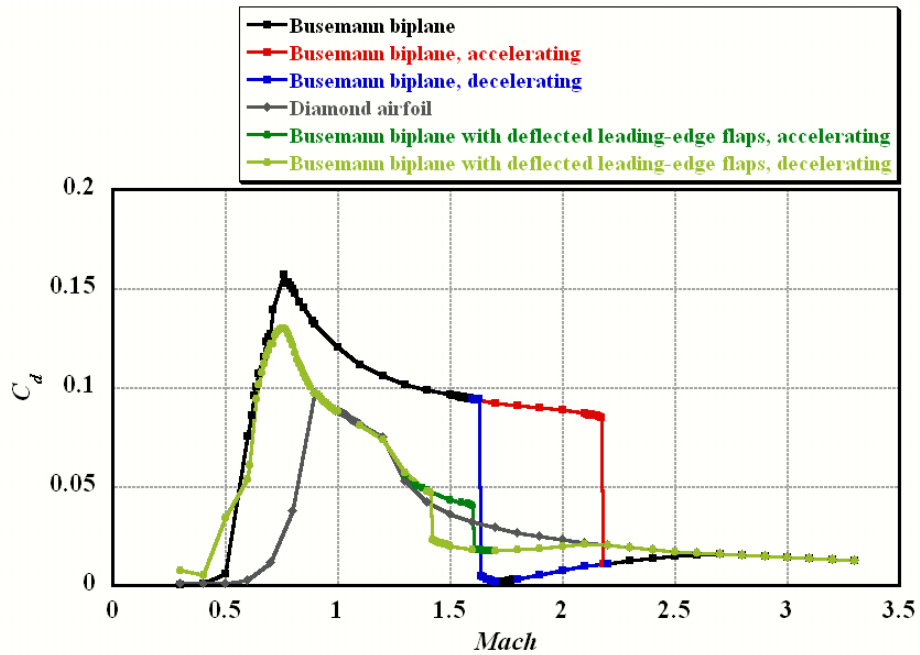


Figure 12. Comparison of the drag characteristics among Busemann biplane, diamond airfoil and Busemann biplane with deflected leading-edge flaps.

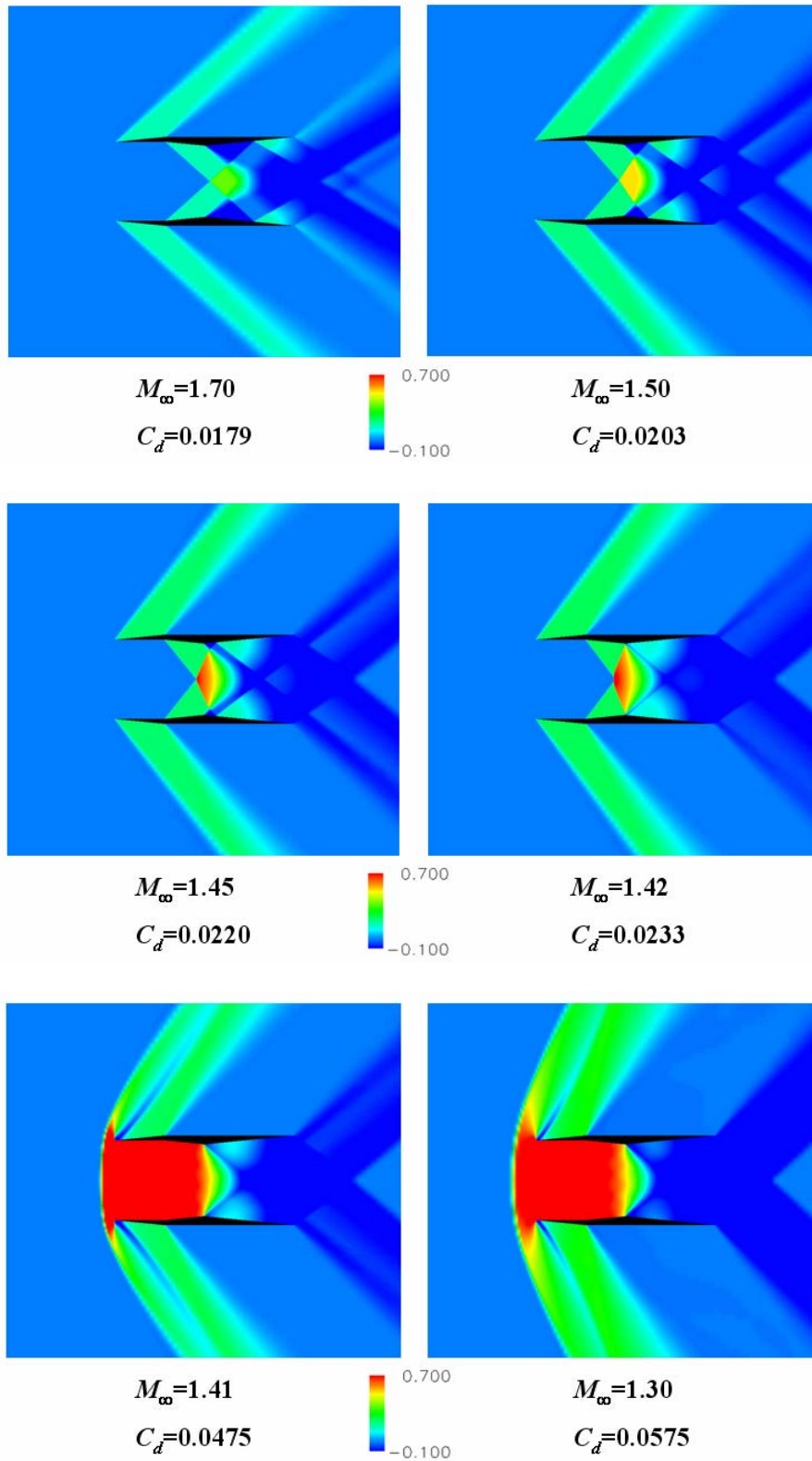


Figure 13.  $C_p$ -contours of Busemann biplane with deflected leading-edge flaps with zero-lift in decelerating condition ( $1.3 \leq M_\infty \leq 1.7$ ).

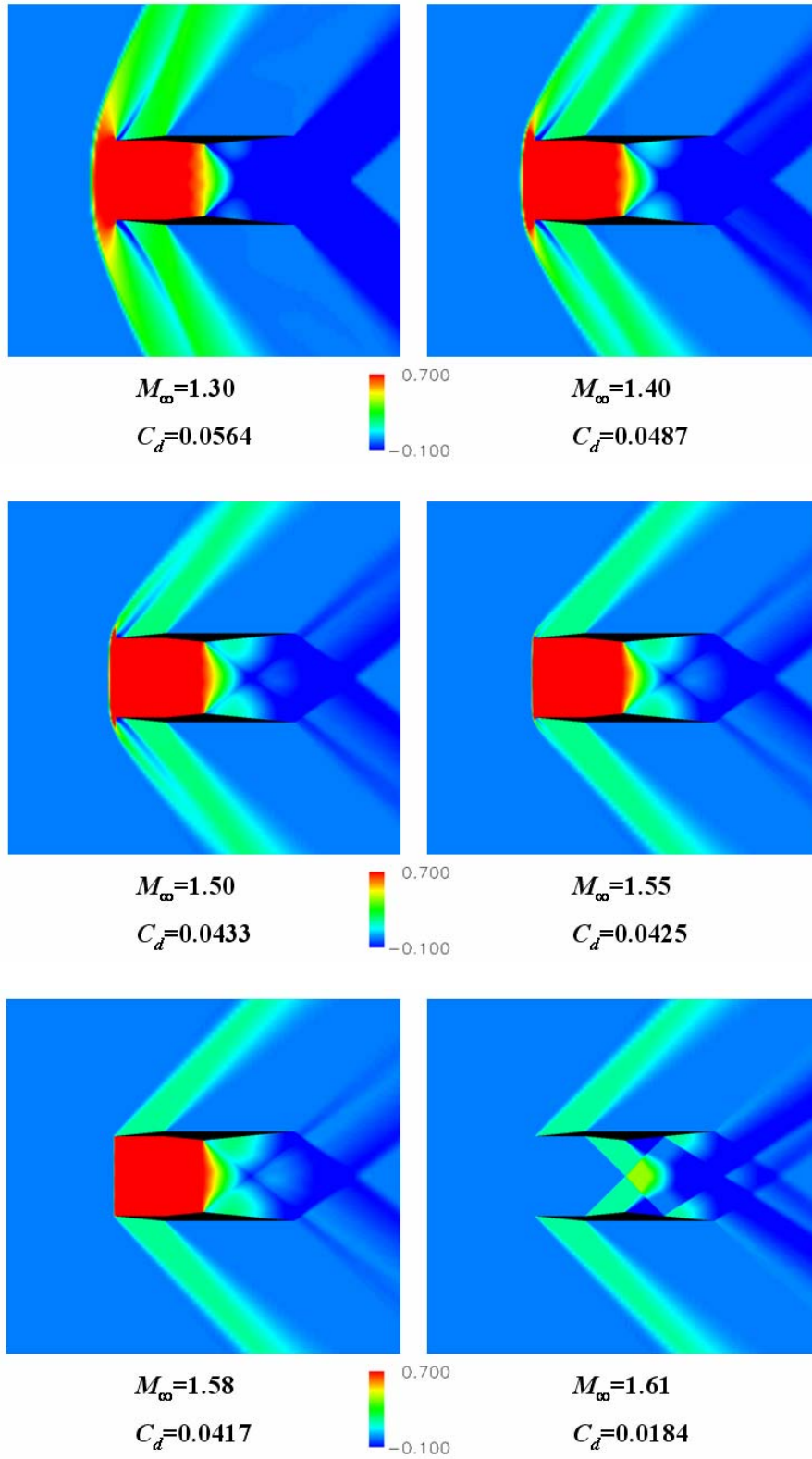


Figure 14.  $C_p$ -contours of Busemann biplane with deflected leading-edge flaps with zero-lift in accelerating condition ( $1.3 \leq M_\infty \leq 1.61$ ).

### C. Busemann Biplane with Deflected Trailing-edge Flaps

In the same way, Busemann biplane with deflected trailing-edge flaps was calculated by considering flow-hysteresis to examine the effect of change in the area of rear streamline on choked-flow and flow-hysteresis. The 28% parts from the trailing-edges of the Busemann biplane ( $t/c=0.05$ ) are moved inward (as sketched in Fig. 15). The inner sides of the deflected parts become parallel to each other. Mach numbers range from 0.3 to 3.3 in inviscid flow mode. The near-field grids are shown in Fig. 16 and the drag characteristics of the biplane are plotted in Fig. 17, which also includes previous results, given in Fig. 3. Pressure coefficient contours around the biplane are plotted in Figs. 18 and 19 with a change in free-stream Mach number.

We can confirm from Fig. 17 that the trailing-edge flaps are not effective in reducing the choked-flow and flow-hysteresis of Busemann biplane. In fact, the increase of  $C_d$  value due to the choked-flow is a little higher than that of Busemann biplane ( $C_d$  value of the biplane is  $C_d=0.1040$  at  $M_\infty=1.63$ , while  $C_d$  value of Busemann biplane is  $C_d=0.0944$  at  $M_\infty=1.63$ ). Also, the area of flow-hysteresis is almost the same as compared to that of Busemann biplane. Here, we would like to focus our attention on the effects of trailing-edge flaps in subsonic flow. Fortunately, we observed from Fig. 17 that wave drags are decreased somewhere between  $M_\infty=0.5$  and  $M_\infty=0.9$  compared to Busemann biplane. These results show that the aerodynamic drag at speed near to or above the speed of sound is reduced, that is, the drag-divergence Mach number is shifted to a higher one. It follows from this that the effect of trailing-edge flaps is useful in downscaling the wave drag in subsonic flow condition.

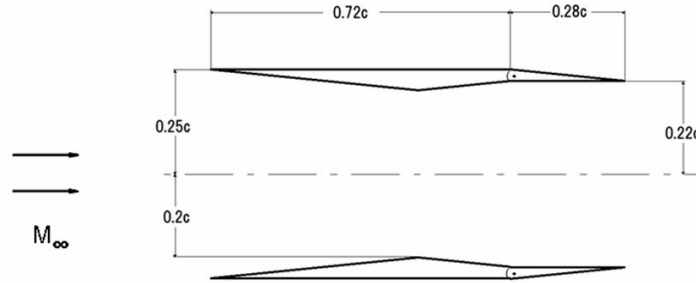


Figure 15. Configuration of Busemann biplane with deflected trailing-edge flaps.

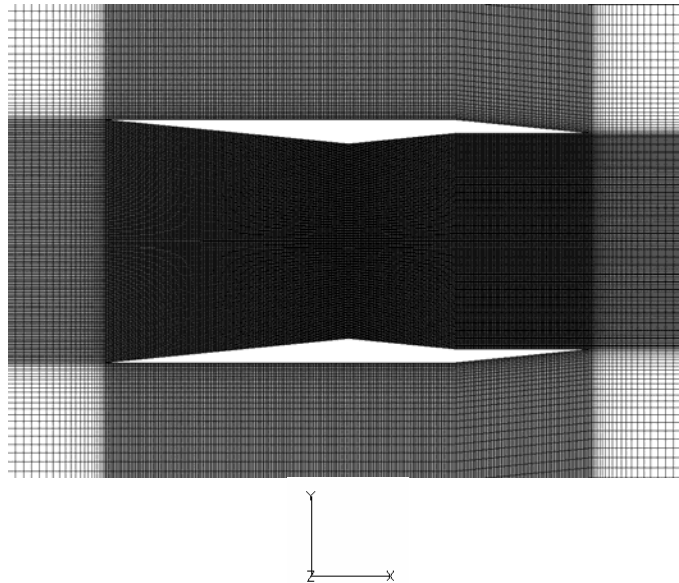


Figure 16. Near-field grids of Busemann biplane with deflected trailing-edge flaps used for UPACS-code analyses.

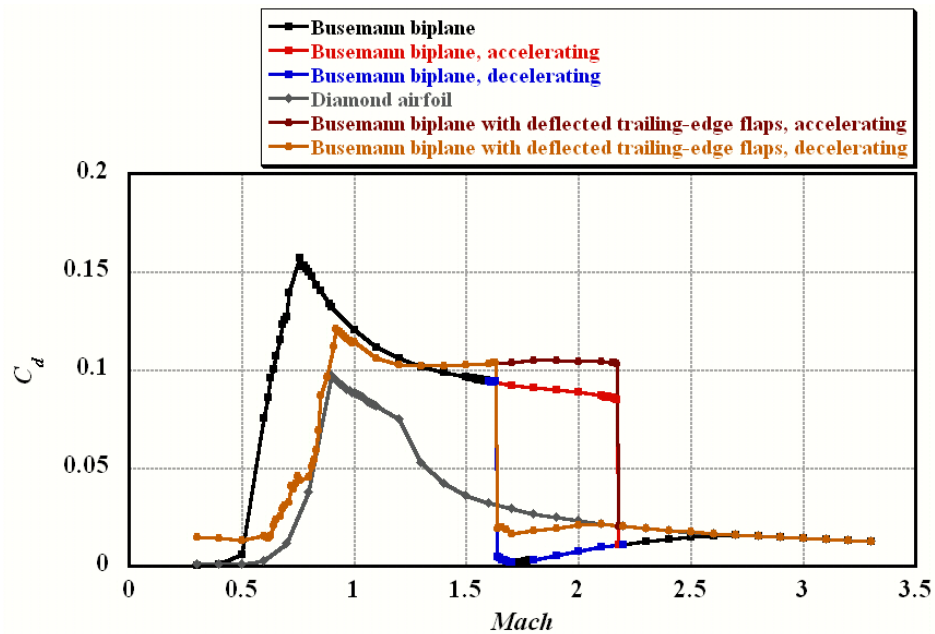


Figure 17. Comparison of the drag characteristics among Busemann biplane, diamond airfoil and Busemann biplane with deflected trailing-edge flaps.

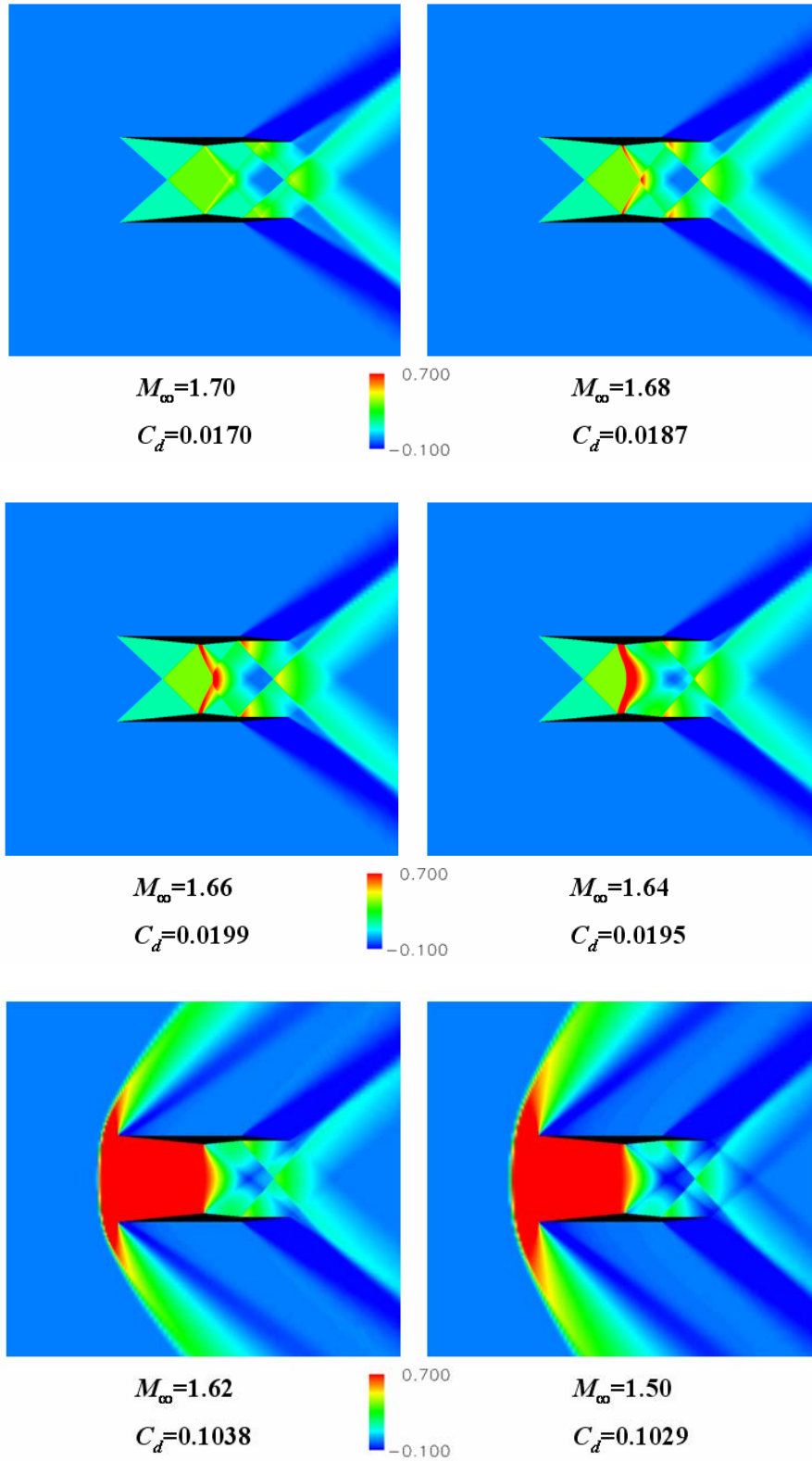


Figure 18.  $C_p$ -contours of Busemann biplane with deflected trailing-edge flaps with zero-lift in decelerating condition ( $1.5 \leq M_\infty \leq 1.7$ ).

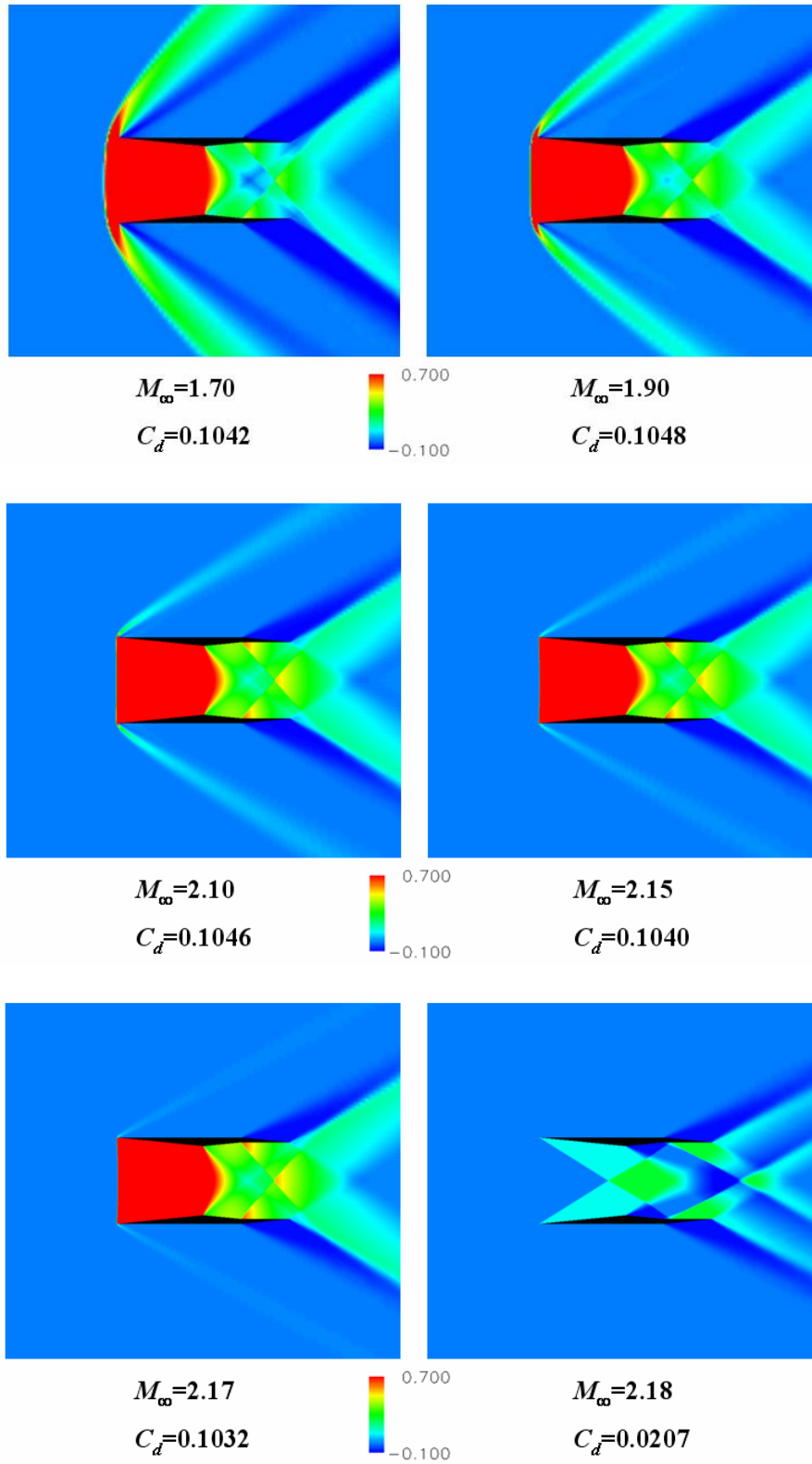


Figure 19.  $C_p$ -contours of Busemann biplane with deflected trailing-edge flaps with zero-lift in accelerating condition ( $1.7 \leq M_\infty \leq 2.18$ ).

#### D. Busemann Biplane with a Combination of Leading- and Trailing-edge Flaps

Finally, we have also designed an airfoil, which has been made by combining Busemann biplane with leading-edge flaps (as shown in Fig. 10) and Busemann biplane with trailing-edge flaps (as shown in Fig. 15) in order to examine the utilization of the effects of each flap. This airfoil is called the HLD-1 (High-Lift Device-1) in this paper (as sketched in Fig. 20). The Euler equation is, similarly, solved using UPACS-code by considering flow-hysteresis over a range of free-stream Mach numbers ( $0.3 \leq M_\infty \leq 3.3$ ), including its design Mach number  $M_\infty=1.7$ . Figure 21 shows the near-field grids of HLD-1. The number of grid points between these two elements are  $251 \times 501$ . The drag characteristics of HLD-1 are plotted in Fig. 22 in comparison with the previous results, given in Fig. 3. Pressure coefficient contours around the HLD-1 are given in Figs. 23 and 24 with a change in free-stream Mach number.

It is clear that the wave drag values of the HLD-1 are close to those of the baseline diamond airfoil at all Mach numbers in Fig. 22. These results suggest that HLD-1 utilize the two effects of the leading-edge flaps and trailing-edge flaps in subsonic and supersonic conditions. Thus, the increase of  $C_d$  due to choked-flow is downscaled and flow-hysteresis area is reduced for a range of Mach numbers ( $1.41 \leq M_\infty \leq 1.6$ , as the  $A_t/A_i$  of HLD-1 is 0.9). In addition, it is easy for HLD-1 to overcome the sound barrier compared to Busemann biplane. Here, we need to pay attention to the fact that the designed Mach number is now set at  $M_\infty=1.7$  in order to use the wave cancellation effect of Busemann biplane for sonic boom suppression. In accelerating condition of HLD-1, the bow shock which is generated in front of the leading-edges is swallowed over at  $M_\infty=1.6$  (by achieving design-condition,  $M_\infty=1.7$ ). Consequently, if the HLD-1 can be transformed into Busemann biplane as Mach number reaches above  $M_\infty=1.6$ , we can arrive at the design point smoothly from subsonic.

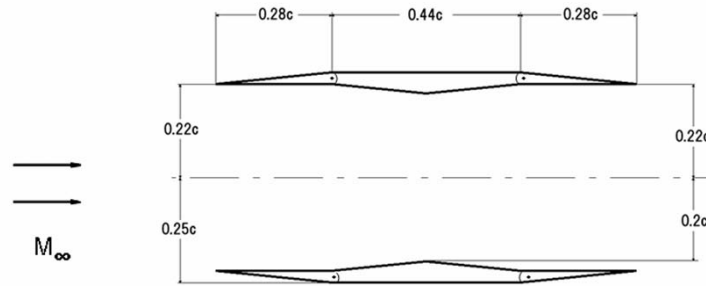


Figure 20. Configuration of HLD-1.

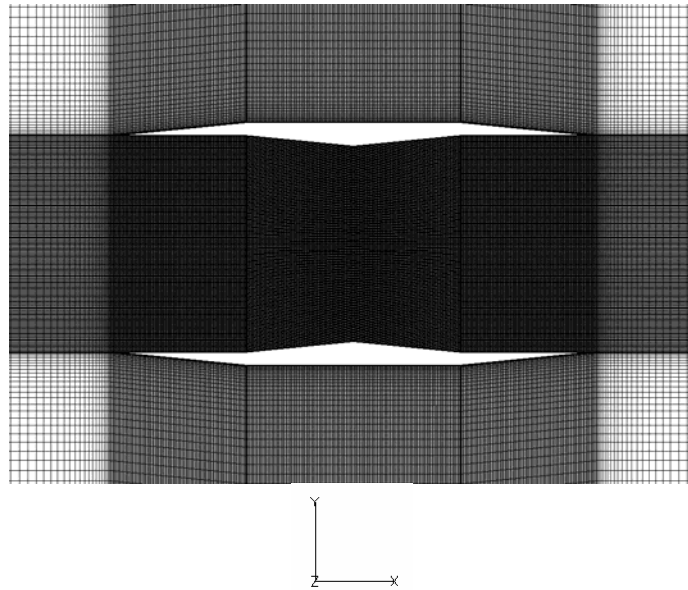


Figure 21. Near-field grids of HLD-1 used for UPACS-code analyses.

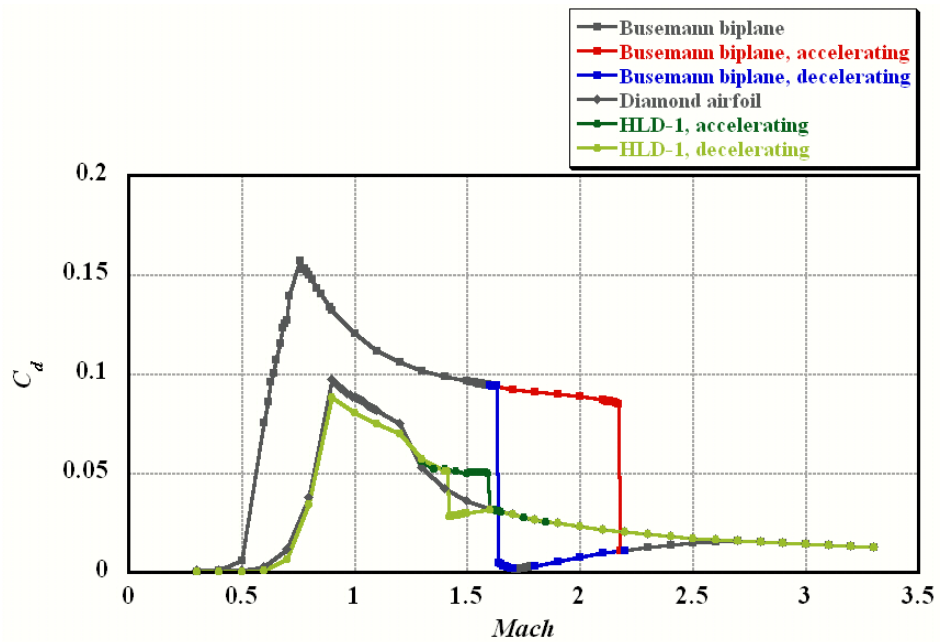


Figure 22. Comparison of the drag characteristics among Busemann biplane, diamond airfoil and HLD-1.

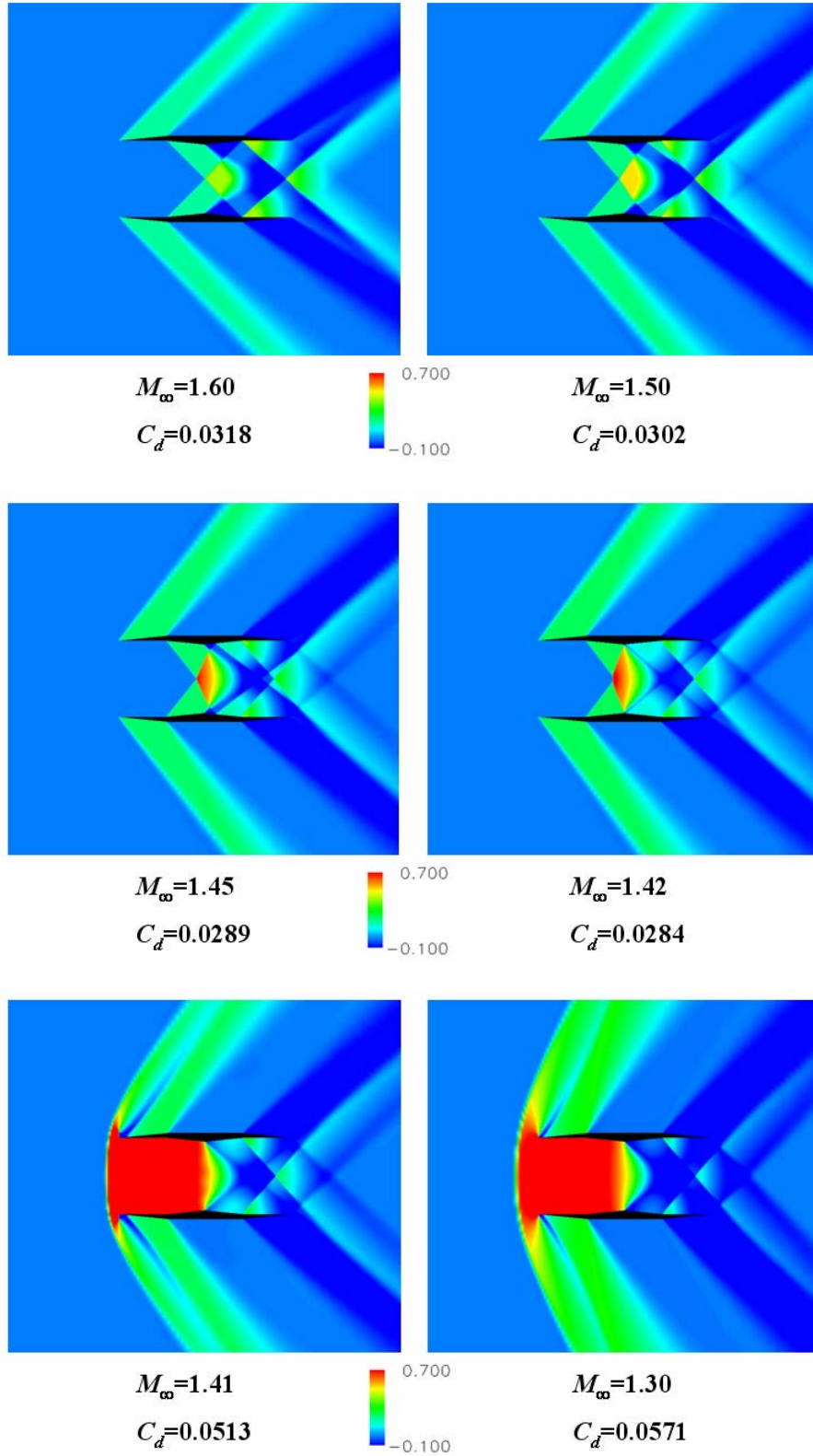


Figure 23.  $C_p$ -contours of HLD-1 with zero-lift in decelerating condition ( $1.3 \leq M_\infty \leq 1.6$ ).

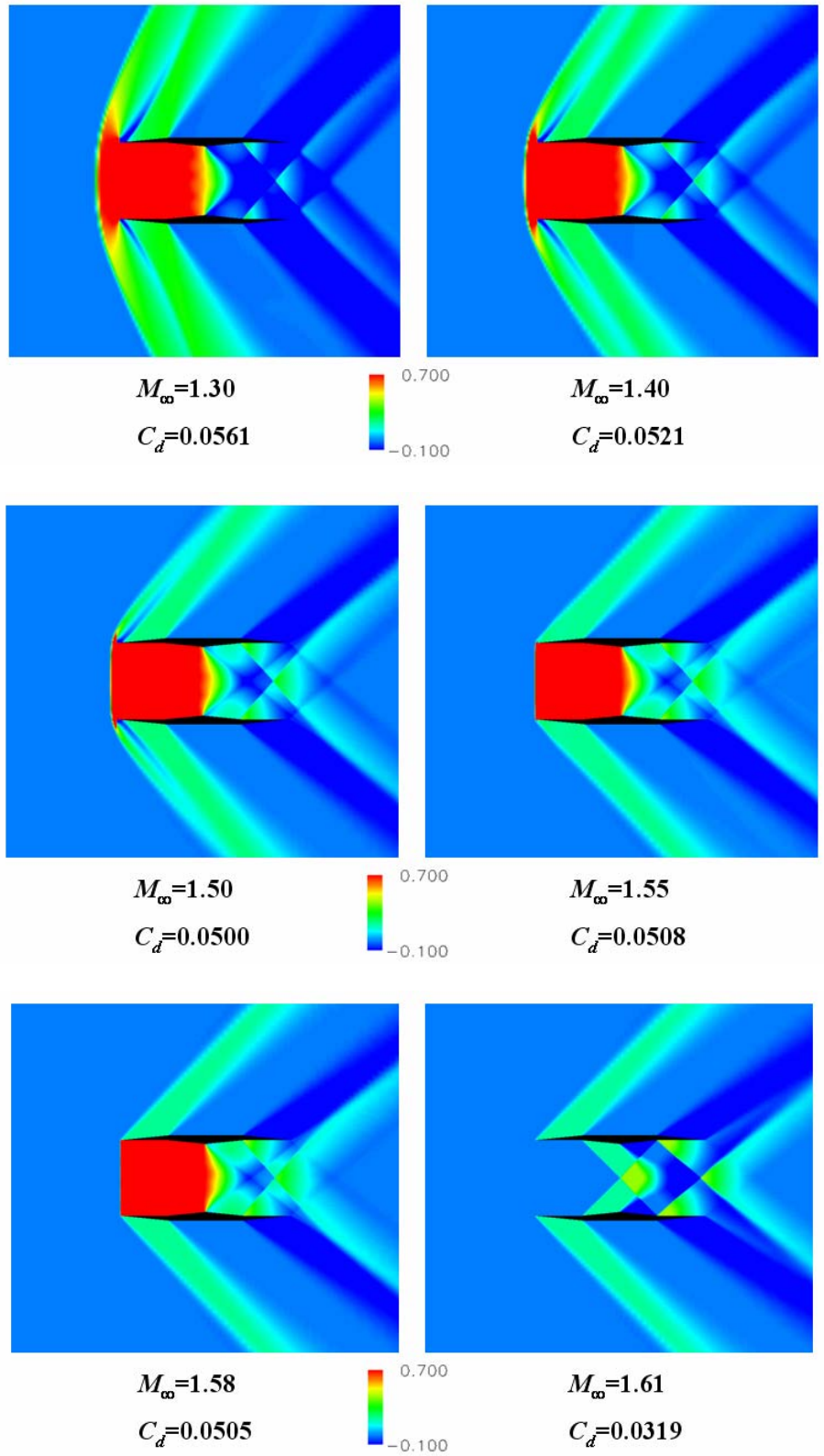


Figure 24.  $C_p$ -contours of HLD-1 with zero-lift in accelerating condition ( $1.3 \leq M_\infty \leq 1.61$ ).

## IV. Conclusion

Three Busemann-type biplanes have been analyzed, focusing on the study of overcoming a choked-flow and flow-hysteresis problems of Busemann biplane using UPACS-code in inviscid flow in 2-D flow condition. These results suggest that the effect of leading-edge flaps, which can change the area of front streamline (the throat-to-inlet-area ratio), can downscale the wave drag in supersonic flow condition, and also some range of subsonic flow conditions. Also, the use of trailing-edge flaps, which can change the area of rear streamline, is useful in downscaling the wave drag in subsonic flow condition, although they are not effective in reducing the choked-flow and flow-hysteresis of Busemann biplane. In addition, it was found that the two effects can be utilized effectively in subsonic and supersonic conditions, by combining the leading- and trailing-edge flaps (like High-lift devices). As a result, the  $C_d$  increase due to choked-flow was downscaled and the area of flow-hysteresis was reduced by using leading-edge flaps. Furthermore, it has become easy to overcome the sound barrier compared to Busemann biplane by using trailing-edge flaps. These are highly possible solutions to these problems. For future works, we need to develop an improved biplane configuration that will not only overcome these problems, but also fulfill a role of high-lift device used at takeoff and landing conditions. For this purpose, we would like to investigate a biplane configuration with plain-flaps that can generate lift enough for low-speed condition.

## Acknowledgments

The author wishes to thank Associate Prof. K. Matsushima of Tohoku University and Visiting Scholar, Dr. M. Kanazaki, of Japan Aerospace Exploration Agency for their invaluable teachings and comments for this research. The author also wishes to gratefully acknowledge my colleagues, especially Ms. J. N. Lim, in publishing this paper. This research was supported by a grant from the Research Fellowships of the Japan Society for the Promotion of Science for young Scientists.

## References

- <sup>1</sup>Kusunose, K., "A New Concept in the Development of Boomless Supersonic Transport," *First International Conference on Flow Dynamics*, Sendai, Japan, November 2004.
- <sup>2</sup>Kusunose, K., Matsushima, K., Goto, Y., Yamashita, H., Yonezawa, M., Maruyama, D. and Nakano, T., "A Fundamental Study for the Development of Boomless Supersonic Transport Aircraft," AIAA Paper, AIAA-2006-0654, January 2006.
- <sup>3</sup>Liepmann, H. W., and Roshko, A., *Elements of Gas Dynamics*, John Wiley & Sons, Inc., New York, 1957, pp.107-123, 389.
- <sup>4</sup>Maruyama, D., Matsushima, K., Kusunose, K. and Nakahashi, K., "Aerodynamic Design of Biplane Airfoils for Low Drag Supersonic Flight," AIAA Paper, AIAA-2006-3323, June 2006.
- <sup>5</sup>Matsushima, K., Maruyama, D., Nakano, T., and Nakahashi, K., "Aerodynamic Design of Low Boom and Low Drag Supersonic Transport using Favorable Wave Interference," *Proceedings of The 36<sup>th</sup> JSASS Annual Meeting*, Tokyo, Japan, April, 2005, pp. 130-133.
- <sup>6</sup>Yamashita, H., Yonezawa, M., Goto, Y., Obayashi, S. and Kusunose, K., "CFD Analyses of Shock Wave Behavior of Busemann's Biplane," *Proceedings of the Aerospace Numerical Simulation Symposium 2005*, JAXA SP-05-017, Feb. 2006, pp.126-131.
- <sup>7</sup>Yamashita, H., "Shock Wave Interaction of Biplane for Realizing a Silent Supersonic Transport," Master Dissertation, System Information Sciences Dept., Tohoku Univ., Sendai, Japan, 2006.
- <sup>8</sup>Van Wie, D. M., Kwok, F. T. and Walsh, R. F., "Starting Characteristics of Supersonic Inlets," *32<sup>nd</sup> AIAA/ASME/SAE/ASEE Joint Propulsion Conference*, AIAA 96-2914, July 1996.
- <sup>9</sup>Takaki, R., Yamamoto, K., Yamane, T., Enomoto, S. and Mukai, J., "The Development of the UPACS CFD Environment," *High Performance Computing, Proc. of ISHPC 2003*, Springer, pp.307-319, 2003.
- <sup>10</sup>Yamashita, H., Yonezawa, M., Goto, Y., Obayashi, S., and Kusunose, K., "Basic Research toward Realizing Boomless Supersonic Aircraft," *Proceedings of the 16<sup>th</sup> Institute of Fluid Science Meeting*, Tohoku University, Sendai, Japan, Dec. 2004, pp. 49-52.